Hyperbaric oxygen treatment on keloid tumor immune gene expression

Chun-Hu Wang[1], Meng-Jie Shan[2,3], Hao Liu[2,3], Yan Hao[2,3], Ke-Xin Song[2], Huan-Wen Wu[4], Tian Meng[2], Cheng Feng[2], Zheng Qi[2], Zhi Wang[2], You-Bin Wang[2]

[1]17th Department of Plastic Surgery, Plastic Surgery Hospital, Chinese Academy of Medical Sciences and Peking Union Medical College, Beijing 100144, China;
[2]Department of Plastic Surgery, Peking Union Medical College Hospital, Beijing 100730, China;
[3]Chinese Academy of Medical Sciences and Peking Union Medical College, Beijing 100730, China;
[4]Department of Pathology, Peking Union Medical College Hospital, Beijing 100730, China.

Abstract

Background: Hyperbaric oxygen treatment (HBOT) has been demonstrated to influence the keloid recurrence rate after surgery and to relieve keloid symptoms and other pathological processes in keloids. To explore the mechanism of the effect of HBOT on keloids, tumor immune gene expression and immune cell infiltration were studied in this work.

Methods: From February 2021 to April 2021, HBOT was carried out on keloid patients four times before surgery. Keloid tissue samples were collected and divided into an HBOT group (keloid with HBOT before surgery [HK] group, $n = 6$) and a non-HBOT group (K group, $n = 6$). Tumor gene expression was analyzed with an Oncomine Immune Response Research Assay kit. Data were mined with R package. The differentially expressed genes between the groups were compared. Hub genes between the groups were determined and verified with Quantitative Real-time PCR. Immune cell infiltration was analyzed based on CIBERSORT deconvolution algorithm analysis of gene expression and verified with immunohistochemistry (IHC).

Results: Inflammatory cell infiltration was reduced in the HK group. There were 178 upregulated genes and 217 downregulated genes. Ten hub genes were identified, including Integrin Subunit Alpha M (*ITGAM*), interleukin (*IL*)-*4*, *IL-6*, *IL-2*, Protein Tyrosine Phosphatase Receptor Type C (*PTPRC), CD86*, transforming growth factor (*TGF), CD80*, *CTLA4*, and *IL-10*. *CD80*, *ITGAM*, *IL-4*, and *PTPRC* with significantly downregulated expression were identified. *IL-10* and *IL-2* were upregulated in the HK group but without a significant difference. Infiltration differences of CD8 lymphocyte T cells, CD4 lymphocyte T-activated memory cells, and dendritic resting cells were identified with gene CIBERSORT deconvolution algorithm analysis. Infiltration levels of CD4 lymphocyte T cell in the HK group were significantly higher than those of the K group in IHC verification.

Conclusion: HBOT affected tumor gene expression and immune cell infiltration in keloids. CD4 lymphocyte T cell, especially activated memory $CD4^+T$, might be the key regulatory immune cell, and its related gene expression needs further study.

Keywords: Keloid; Hyperbaric oxygen treatment; Tumor immune gene; Immune cell

Introduction

Keloids are a kind of skin fibroproliferation disease with tumor-like characteristics. Studies on the pathologic mechanism of this disease have been reported in the literature.[1-9] The widely explored fields include genetics, inflammation, immunology, oncology, etc. In a genetic study, Marneros *et al*[1,2] reported 14 keloid families and loci on chromosomes 2q23 and 7p11. Inflammatory factors have been deeply studied. The reported inflammatory factors include interleukin (IL)-1,[3] IL-6,[3] tumor necrosis factor (TNF)-α,[3] IL-10,[4] IL-4,[5] and IL-13.[5] Bloch *et al*[6] reported general immune reactivity in patients with keloids in 1984. The roles of macrophages and lymphocyte T cells have been discussed over the years.[7] The tumor-like characteristics of keloids encourage many studies in view of oncological mechanisms. Lee *et al*[8] reported that the STAT3 signaling pathway is implicated in keloid pathogenesis. STAT3 protein plays an important role in cancer and inflammation.[9] These studies demonstrate that keloid development is a complicated process and that many factors, such as genes, inflammation, and immunity, are involved. The combined effects of these factors may result in skin tumor-like fibroproliferation after injury. Tumor immune genes and related immune cells may be involved in the process of keloid development.

Access this article online

Quick Response Code:

Website: www.cmj.org

DOI: 10.1097/CM9.0000000000001780

Chun-Hu Wang and Meng-Jie Shan contributed equally to this work.

Correspondence to: You-Bin Wang, Department of Plastic Surgery, Peking Union Medical College Hospital, Beijing 100730, China
E-Mail: wybenz@sina.com

Chinese Medical Journal 2021;134(18)
Received: 05-07-2021 **Edited by:** Ning-Ning Wang

Hyperbaric oxygen treatment (HBOT) has been widely used in clinical practice. Song *et al*[10] first reported its effect on keloid treatment. They found that the recurrence rate was lower in the group with HBOT than in the group without HBOT. More studies on the effects of HBOT on the keloid development process have been reported. The effects of HBOT on keloid Epithelial-Mesenchymal Transition (EMT) have been discussed in a report by Zhang *et al*.[11] They found that HBOT can ameliorate the EMT of keloid tissue. It has been found that HBOT can relieve pruritus and pain in patients with keloids.[12] The effects of HBOT on inflammatory factors were reported by Hao *et al*.[13] Keloid tissue with HBOT demonstrated lower IL-12p40 expression and higher IL-1 receptor antibody (IL-1Ra) expression. These studies verified the effects of HBOT on keloid development. Some pathologic mechanisms have also been explored in these studies, but the molecular biologic mechanism is far from understood, especially the mechanism of tumor immune gene expression and related immune cell infiltration. In this study, keloid tissue tumor immune gene expression and related immune cell infiltration after HBOT were explored, and their roles in keloid development and the HBOT process were discussed.

Methods

Ethical approval

This study was approved by the Medical Ethics Committee of Peking Union Medical College Hospital (No. JS-2907). Written informed consent was obtained from all participants.

Sample collection

From February 2021 to April 2021, a total of 12 patients (patients with keloids who had undergone HBOT before surgery and those who had not undergone HBOT) participated in this study. The patients were diagnosed with no systemic disease and took neither medication nor other treatments (such as corticosteroids or 5-fluorouracil injections or radiotherapy) before this study. The basic demographic information (sex and age) of patients was collected, and the modified Vancouver Scar Scale was used to assess the condition of keloids according to the type of keloid lesion. The age of the patients ranged from 22 to 47 years. All samples were taken from the chest. The keloid sample was taken from the keloid tissue removed during surgery.

The collected specimens were divided into two groups: the group with keloid tissue without HBOT (K group, $n = 6$) and the group with keloid tissue with HBOT before surgery (HK group, $n = 6$). Six keloid tissue samples in each group were randomly collected.

HBOT methods

HBOT was carried out four days before surgery (once a day, four times in total) in an air pressure medical hyperbaric chamber with three locks and seven doors. The pressure was increased to 0.2 MPa (2 atmosphere absolute [ATA]) at a constant speed within 30 min. When the pressure reached the stable value, patients inhaled 100% oxygen through face masks. Oxygen treatment continued for 60 min. Then, the chamber pressure was decreased to normal within 30 min, and the patients left the chamber. Keloid surgery was performed within 24 h after the last HBOT.

Tumor immune-related gene expression level

An Oncomine Immune Response Research Assay (Thermo Fisher, USA) kit was used to analyze the expression of tumor immune-related genes. This is an ribonucleicacid (RNA)-based multitarget sequencing kit. It can measure the expression levels of 395 genes related to immune response and tumor immunity in 36 functional annotation groups. All the experimental operations were carried out under the instructions of the product.

Differential gene screening and annotation

The threshold was set to a $P < 0.05$ and log2-fold change (FC) >1.5 or < -1.5. The R package software version 3.4.3 (R Foundation for Statistical Computing, Vienna, Austria) was used to create scatter plots. The R package was used to perform functional annotations on differentially expressed genes (DEGs) for biological processes (BPs), cell components (CCs), molecular functions (MFs), and Kyoto Encyclopedia of Genes and Genomes (KEGG).

Construction of protein interaction network

STRING (V11.5; http://string-db.org), a search tool for searching interacting genes, can convert differentially transcribed genes into expressed proteins and construct a protein–protein interaction (PPI) network. The PPI network of common DEGs was obtained through STRING and visualized with Cytoscape (version 3.7.2, Cytoscape Consoritum, USA).

Identification of the expression of hub genes

CytoHubba is a plug-in for Cytoscape that is used to identify important modules in the PPI network. CytoHubba was used to screen out the top ten core genes from the PPI network.

Hub genes verification with qPCR

Skin tissues (K and HK groups) were extracted from the same patient for PCR verification. The primers used in this study are shown in Table 1. A total of 200 mg of tissue was mixed with TRIzol (Thermo Fisher, USA) reagent to extract total RNA using a one-step method. A ultraviolet spectrophotometer produced by Eppendorf was used to test the purity and content, and then, 1 μg of total RNA was removed. A reverse transcription kit was used to reverse transcribe cDNA (HiScript III 1st Strand cDNA Synthesis Kit, Beijing, China). Then, a qPCR fluorescence kit (Taq Pro Universal SYBR qPCR Master Mix) was used to quantitatively analyze the expression of the target gene. The reaction system was 10 μL 2 × Taq Pro Universal SYBR qPCR Master Mix + 0.4 μL Gene Specific Primer

Table 1: Primers and their sequences for PCR analysis.

Primer	Sequence (5′–3′)
GAPDH-F	GGAAGCTTGTCATCAATGGAAATC
GAPDH-R	TGATGACCCTTTTGGCTCCC
IL-10-F	TACCACCTCCCGAAAATGTCA
IL-10-R	CCCAGTCTGAATGCTCATCTG
CTLA-4-F	GCCCTGCACTCTCCTGTTTTT
CTLA-4-R	GGTTGCCGCACAGACTTCA
CD80-F	GGCCCGAGTACAAGAACCG
CD80-R	TCGTATGTGCCCTCGTCAGAT
CD86-F	CTGCTCATCTATACACGGTTACC
CD86-R	GGAAACGTCGTACAGTTCTGTG
IL-4-F	CCAACTGCTTCCCCCTCTG
IL-4-R	TCTGTTACGGTCAACTCGGTG
IL-6-F	ACTCACCTCTTCAGAACGAATTG
IL-6-R	CCATCTTTGGAAGGTTCAGGTTG
IL-2-F	ACCGCTTTGCGGAATCTCA
IL-2-R	AGGTCAGGGAAACATCAGGGA
PTPRC-F	TTGAGCGACAGGAGGATGAG
PTPRC-R	GACGCCTCTCCACATTGCT
ITGAM-F	ACTGGTGAAGCCAATAACGCA
ITGAM-R	TCCGTGATGACAACTAGGATCTT
TGF-F	GACAAGGTGTACGTGAACATCG
TGF-R	CCACACTGTGTCGCCGTAG

IL: Interleukin; TGF: transforming growth factor.

Forward (10 μM) + 0.4 μL Gene Specific Primer Reverse (10 μM) + 1 μL cDNA + 9.2 μL RNase-free double distilled H_2O. The reaction conditions were 95°C for 30 s during before denaturation, 95°C for 3 s, and 60°C for 10 s for 40 cycles; the reaction conditions were 95°C for 15 s, 60°C for 60 s, and 95°C for 15 s after denaturation; the amplification curve was obtained at the end of the run.

Immune cell infiltration analysis

CIBERSORT deconvolution algorithm is a machine learning method based on linear support vector regression and is highly robust to noise. Through the CIBERSORT deconvolution algorithm, the gene expression information was transformed into the proportion information of immune cells.

Immune cell infiltration verification with immunohistochemistry (IHC)

The HE sections of the skin wax block were further labeled by IHC. Immunohistochemical staining was performed using the Envision two-step method. Antibodies for CD8 T cell, CD4 T cell, and CD1a dendritic cells were operated in accordance with the instructions. The CD4 (67786-1-Ig), CD8 (66868-1-Ig), and CD1a (17325-1-AP) antibodies were all purchased from ProteinTech (Chicago, USA). The stained cells were calculated using Image J (1.8.0.112; version 2.1.4.7, National Institutes of Health, Maryland, USA) to get the quantitative results.

Statistical analysis

Statistical analysis was performed using SPSS software version 22.0 (IBM Corporation, Armonk, NY, USA), and a P of <0.05 was considered statistically significant. The t test was used to test whether the average difference between the two groups was significant.

Results

Histological characteristics of the K and HK groups

HE staining was applied to the samples. The characteristics of keloid skin from patients with keloids are displayed in Figure 1A. The characteristics of keloid skin from patients with keloids undergoing HBOT before surgery are displayed in Figure 1B. Obvious inflammatory cell aggregation around microvessels was also displayed in keloid tissue without HBOT [Figure 1A and 1B].

Data quality evaluation

To understand the distribution of data intuitively, principal component analysis was used to perform dimensionality reduction analysis on the data. The samples of the K and HK groups were divided into two groups [Figure 2A].

Identification of DEGs and data mining

There were 178 upregulated genes and 217 downregulated genes between the K group and the HK group. DEGs were used to construct a PPI network [Figure 2B]. Cytoscape software was used to further identify the most important hub gene network [Figure 2C].

Functional annotation of DEGs by gene ontology (GO) and KEGG analyses

The screening criteria for GO and KEGG analysis were log2-FC >1.5 or <-1.5 and $P<0.05$. GO analysis included BPs, CCs, and MFs. BP analysis showed T-cell activation and regulation of lymphocyte activation in the K group as compared to that in the HK group [Figure 3A]. Variations in CCs were markedly enriched on the external side of the plasma membrane [Figure 3B]. Variations in MFs were markedly enriched in cytokine activity and cytokine receptor binding [Figure 3C]. Analysis of KEGG pathways in the K group compared with the HK group demonstrated infection with influenza A, cytomegalovirus, and Kaposi sarcoma-associated herpesvirus infection [Figure 3D].

Hub gene expression

Primers designed for hub genes in the K group as compared to those in the HK group included *CD80*, *CD86*, *CTLA4*, *IL-2*, *IL-4*, *IL-6*, *IL-10*, *ITGAM*, *PTPRC*, and transforming growth factor (*TGF*) [Table 1]. Among the identified genes, *CD80, IL-4, ITGAM, and PTPRC* decreased significantly in the HK group as compared with those in the K group ($P<0.05$). *CTLA4*, *IL-6*, *CD86*, and *TGF* decreased in the HK group as compared to those in the K group, but there was no significant difference. *IL-10* and *IL-2* levels were increased in the HK group compared to those in the K group, but there was no significant difference [Figure 4A-D].

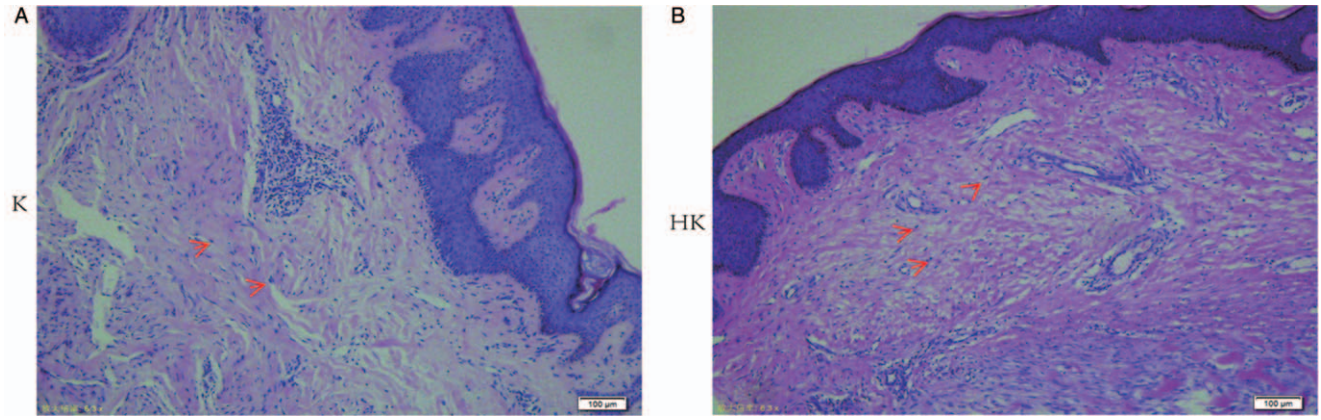

Figure 1: Histological images (H & E) of the K group (A) and HK group (B). Obvious squamous epithelium and fibroblast hyperplasia were observed in (A) compared with (B) with obvious inflammatory cell aggregation around microvessels. K: non-HBOT group; HK: HBOT group; H&E: hematoxylin-eosin staining.

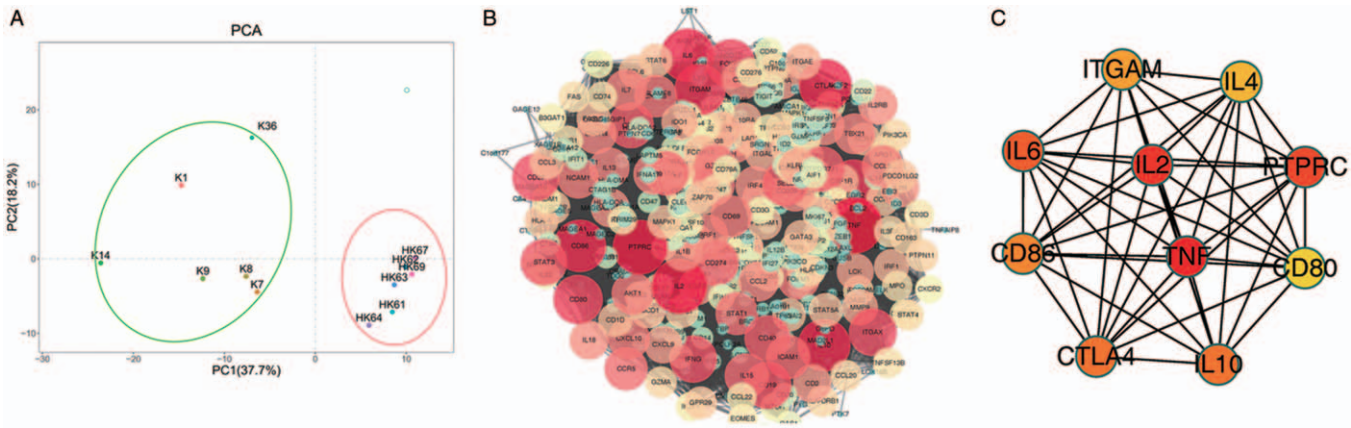

Figure 2: PCA of samples between groups K and HK (A). PC1 and PC2 are used as the X-axis and Y-axis, respectively, to draw the scatter diagram, where each point represents a sample. In such a PCA diagram, the farther the two samples are from each other, the greater the difference is between the two samples in gene expression patterns. The PPI network of DEGs in groups K and HK (B). The hub genes were identified from the PPI network in groups K and HK (C). DEGs: Differentially expressed genes; PC1: Principal component 1; PC2: Principal component 2; PCA: Principal component analysis; PPI: Protein-protein interaction.

Immune cell infiltration analysis

Through the CIBERSORT deconvolution algorithm, the gene expression information was transformed into the information of the proportion of immune cells. Then, through the histogram, heat map, and violin map, the visual analysis showed that there were differences in various immune cells between the two groups [Figure 5A–C]. CD8 lymphocyte T-cell infiltration decreased significantly in the HBO group. CD4 lymphocyte T-activated memory cell and dendritic resting cell infiltration increased significantly in the HBO group.

Immune cell infiltration verification with IHC

IHC was used for immune cell staining, and significant differences in the CD4 lymphocyte T cell were found between the two groups ($P < 0.05$). CD8 lymphocyte T cells and CD1a dendritic cells were slightly higher in the HBO group but without significance [Figure 6A–C].

Discussion

There are many factors influencing keloid scar formation. The most emphasized factors include ethnicity, genetic predisposition, sex, age, body site, and environmental factors such as trauma and infection.[14] Keloid formation is most likely to occur after an inciting stimulus, such as dermal injury or inflammatory process, at a keloid-prone anatomical site in a genetically predisposed individual.[15] Abnormal genetic expression, immune cell reaction, and inflammation result in abnormal behavior of related cells, such as myofibroblasts, fibroblasts, keratinocytes, endothelial cells, and nerve cells, in this process and ultimately cause keloid formation, which is a type of incomplete malignancy that has undergone some, but not all, tumorigenic changes.[16] However, the mechanisms behind this process are still poorly understood. Because of this, keloid management is far from satisfactory.

The reported keloid treatment methods include occlusive dressings, compressive therapy, intralesional steroids, topical imiquimod, topical mitomycin C, intralesional and topical 5-fluorouracil (5-FU), interferons, bleomycin, surgical techniques, cryotherapy, radiation therapy, pulsed dye laser, ablative laser, laser-assisted drug delivery, etc. As an auxiliary treatment method, HBOT was first introduced by Song *et al*.[10] In their report, the recurrence rate was

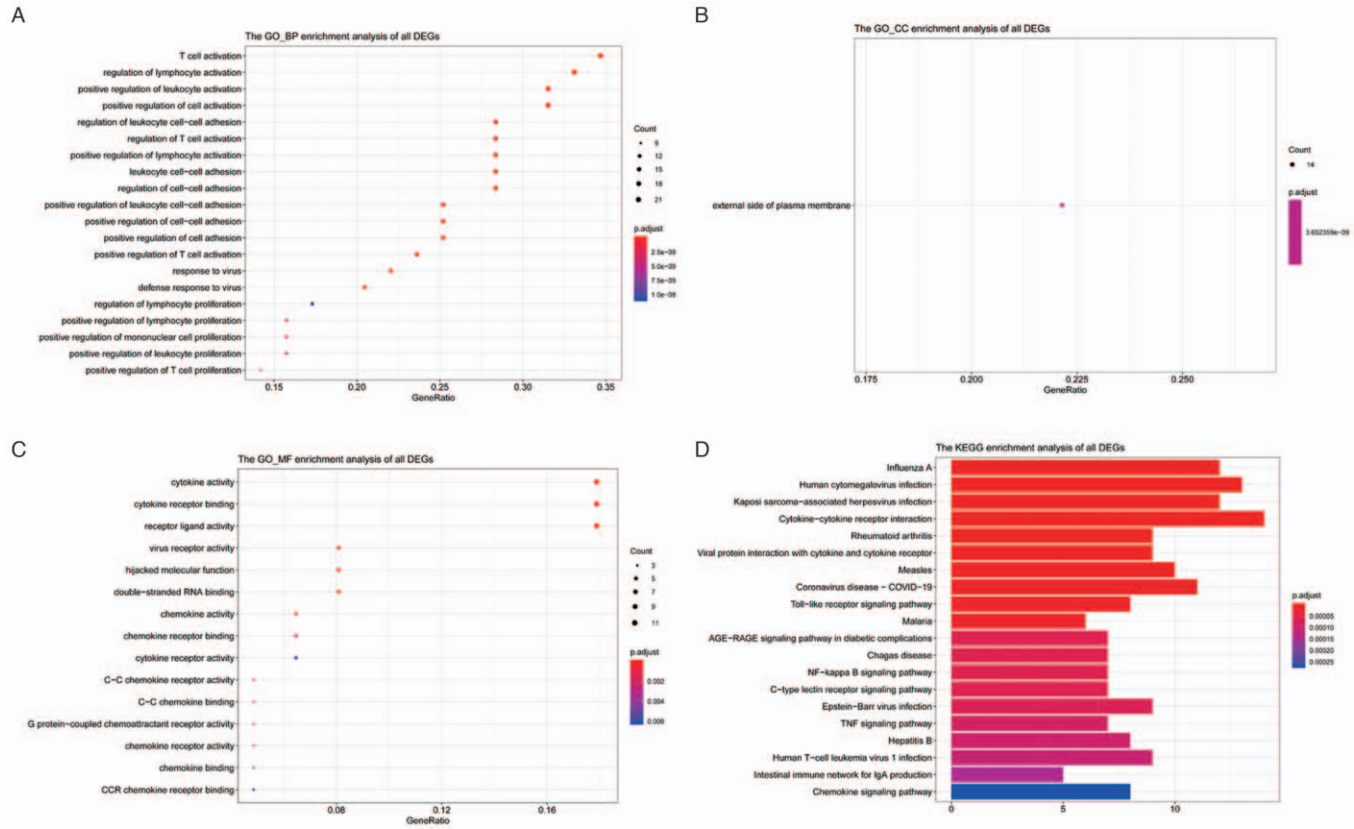

Figure 3: GO enrichment analyses of BP, CC, and MF of DEGs between groups K and HK (A–C). BP analysis showed that T-cell activation and regulation of lymphocyte activation in the K group as compared to that in the HK group (A). Variations in CCs were markedly enriched on the external side of the plasma membrane (B). Variations in MFs were markedly enriched in cytokine activity and cytokine receptor binding. The cutoff for log2 FC >1.5 or <-0.5 and $P<0.05$ were used as screening criteria (C). KEGG pathway analysis of DEGs between groups K and HK. (D). BP: Biological processes; CCs: Cell components; DEGs: Differentially expressed genes; FC: Fold change; GO: Gene ontology; MF: Molecular functions.

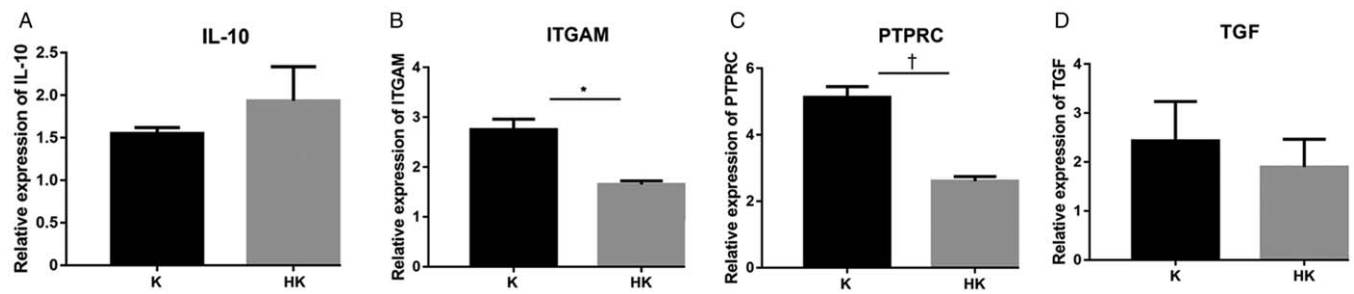

Figure 4: Primers designed for hub genes in the K group ($n=6$) as compared to those in the HK group ($n=6$) included IL-10 (A), ITGAM (B), PTPRC (C), and TGF (D). Relative expression of IL-10, ITGAM, PTPRC, and TGF by RT-qPCR analysis. IL-10 levels were increased in the HK group compared to those in the K group, but there was no significant difference. IL: Interleukin. Protein Tyrosine Phosphatase Receptor Type C (PTPRC), transforming growth factor (TGF). $^{*}P<0.05$, $^{\dagger}P<0.01$.

reduced from 14.15% to 5.97% after HBOT, and the difference was significant. HBOT was later reported to reduce the pruritus and pain symptoms of the patient.[12] The molecular biologic effects of HBOT on keloids were also studied. Zhang *et al*[11] found that HBOT can ameliorate the keloid EMT process by influencing hypoxia inducible factor-1α(HIF-1α) expression. In addition, HBOT can also influence the expression of inflammatory factors, such as IL-12p40, macrophage inflammatory protein-1β(MIP-1β), Platelet derived growth factor (PDGF-BB), and IL-1R. They found that HBOT significantly decreased the expression levels of IL-12p40, MIP-1β, and PDGF-BB and increased the expression level of IL-1Ra.[13] These studies indicate that HBOT may widely affect keloid pathophysiological processes, and deep exploration of its mechanism is needed.

In this study, the mechanism of HBOT in keloids was explored in view of tumor immune gene expression. A total of 178 genes were upregulated and 217 genes were downregulated in keloid tissue after HBOT. The ten hub genes included *ITGAM*, *IL-4*, *IL-6*, *IL-2*, *PTPRC*, *CD86*, *TNF*, *CD80*, *CTLA4*, and *IL-10*. Of these, *CD80*, *ITGAM*, *IL-4*, and *PTPRC* were identified with significant downregulated expression. *CTLA4*, *IL-6*, *CD86*, and *TGF* were also identified to have downregulated expression, but

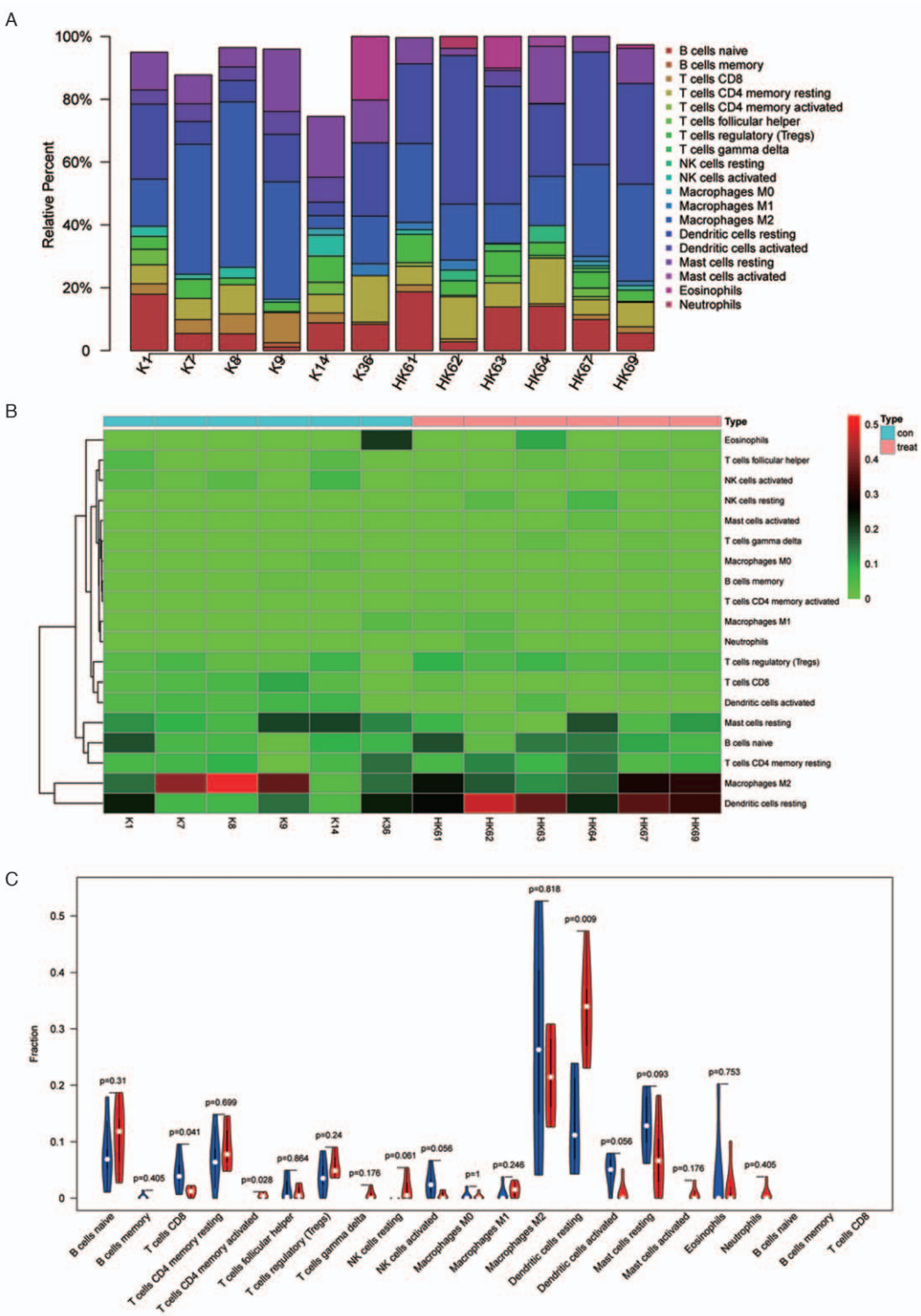

Figure 5: The histogram, heat map, and violin map of immune cell analysis between the two groups with CIBERSORT deconvolution algorithm (A–C). Differences of CD8 lymphocyte T cell, CD4 lymphocyte T-activated memory cell, and dendritic resting cell between the two groups were displayed.

there was no significant difference. *IL-10* and *IL-2* were upregulated, but there was no significant difference. CD80 and CD86 are T lymphocyte activation antigens. They participate in T lymphocyte proliferation and IL-2 production after binding with CD28 or CTLA-4.[17] ITGAM encodes the α-chain subunit of heterodimeric integrin-αMβ2. It is a cell surface receptor expressed primarily on monocytes and neutrophils. Its functions include inactivation, adherence, and migration of leukocytes by stimulated endothelium, phagocytosis of complement-coated particles, and neutrophil apoptosis.[18] Produced mainly by Th2-polarized T cells, IL-4, and IL-13 are short α-helix bundle glycoproteins with approximately 30% homology. IL-4 and IL-13 can promote

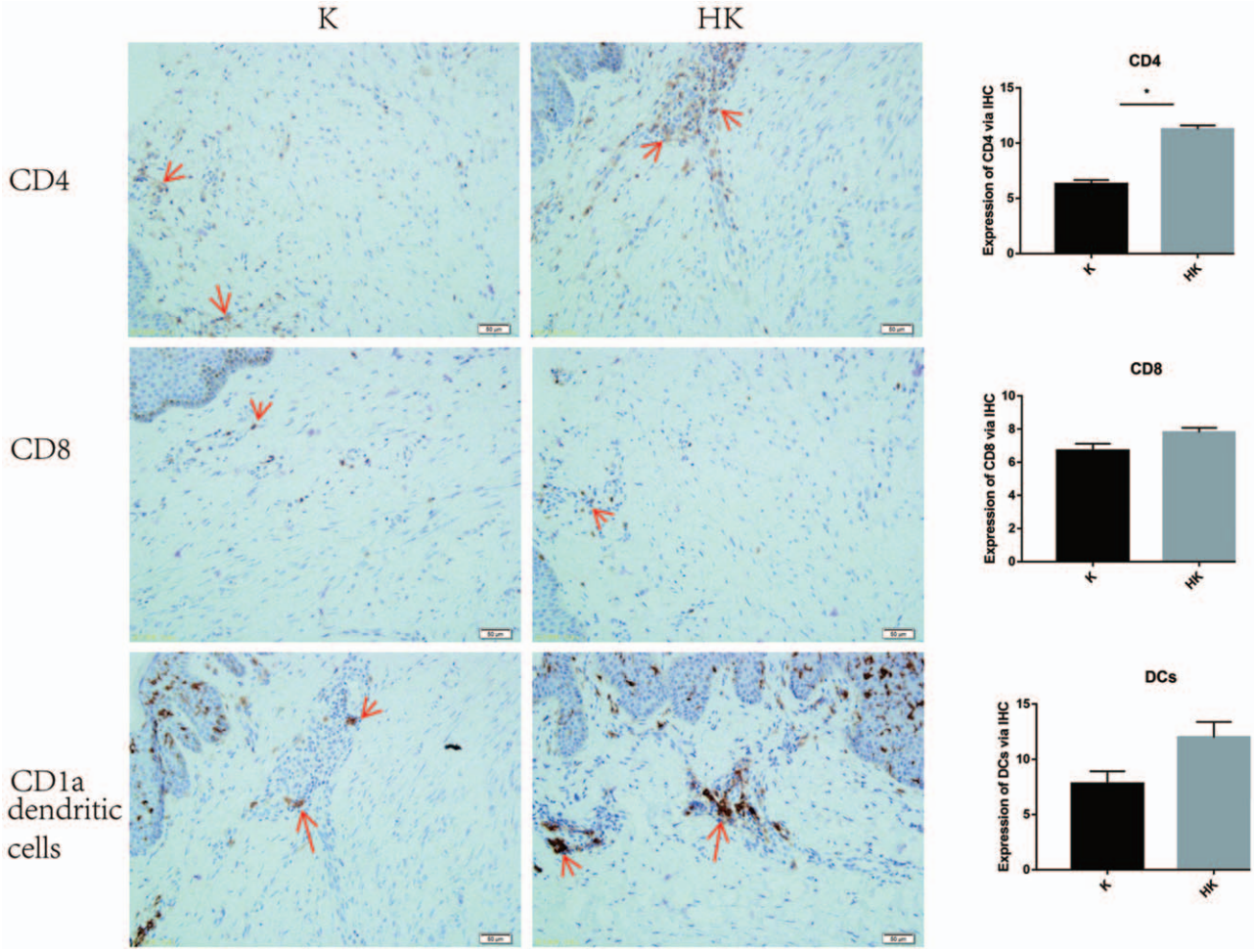

Figure 6: IHC verification of CD8 lymphocyte T cell, CD4 lymphocyte T cell, and CD1a dendritic cell. Significant differences in CD4 lymphocyte T cell were found between the two groups ($P < 0.05$). IHC: Immunohistochemistry; Arrows indicate positive results for antibodies.

fibroblast chemotaxis and proliferation, myofibroblast differentiation, and the production of collagen and extracellular matrix macromolecules.[19] PTPRC is a CD45 antigen. It is a transmembrane receptor-like molecule expressed on many immunorelevant cells. PTPRC is an important TNF signaling molecule. It regulates signaling thresholds in immune-related cells.[20] TGF-dependent signaling is associated with fibroblast proliferation and myofibroblast differentiation. Its expression is crucial for tissue scarring and collagen synthesis.[21] IL-6 and IL-17 were reported to be significantly increased in keloids with a proinflammatory function. IL-10 has been reported to significantly inhibit the proliferation of keloid fibroblasts by the TGF-β/Smad pathway. Faleo *et al*[22] found in a mouse diabetic model that HBOT can reduce T-cell proliferation and the co-stimulation markers DC80 and CD86. Song *et al*[10] reported that the expression of IL-6 in the HBOT group was significantly lower than that in the control group. The protective effect of HBOT on sepsis relies on IL-10 expression.[23] Anti-inflammatory effects of HBOT have also been reported in neurological models, such as Alzheimer disease. Anti-inflammatory cytokines, such as IL-4 and IL-10, were demonstrated to have increased expression after HBOT.[24] These results suggest that HBOT can regulate some immune gene expression in the keloid tissue environment. There are no reports about the effects of HBOT on ITGAM and PTPRC in the literature. Their relationship needs further study.

Many studies demonstrated that immune cells play an important role in keloid development. The role of macrophage and T lymphocyte has been reported and discussed in literatures.[7,25] Mast cells were also suggested to be an important type of immune cell in keloid development.[26] Macrophage is suggested as a type of fibrosis-promoting cell because of the role of its M2 phenotype in fibrosis, but the role of T lymphocyte is more complex.[25] Little conclusion regarding the roles of T-cell subtypes in scar formation has yet been known.[25] Positive correlation between mast cells and the degree of scar have been demonstrated in literature.[26-28]

No study been reported about the effect of HBO treatment on keloid immune cell infiltration in the literature. Our study demonstrated that there were no significant differences in macrophage fraction in any phenotype between the HK and K groups. So, it was with mast cells. A fraction of $CD8^+$T cells in the K group was significantly higher than that in the HK group in immune cell infiltration analysis results. But in IHC verification, the observed $CD8^+$T cells

in the K group were little lower than those in the HK group without significant differences. Further verification studies are needed. A fraction of resting dendritic cells was significantly higher in the HK group in immune cell infiltration analysis results, but the differences between the two groups were not significant in the IHC verification study. A fraction of activated memory $CD4^+$T cells was significantly higher in the HK group in immune cell infiltration analysis results. A significant increase of $CD4^+$T cells in the HK group was also observed in IHC verification. These results suggest that $CD4^+$T cells, especially activated memory $CD4^+$T, may be the key regulatory immune cell in HBOT-induced keloid immune cell infiltration transformation. Its role and mechanism in this process need further study.

The limitations of this study include the following: (1) the experimental samples were small. Only six patients in each group were included in this study, and the deviation in the results was large. More patients will need to be studied in the future. (2) HBOT time was relatively short. The HBOT group only received four treatments before surgery. The influences of HBO on keloid tissue might not reach such a deep level that many other significant changes could be detected. Long-term HBOT studies will need to explore more complicated influences. (3) This study only verified some key tumor immune genes and related key regulatory immune cells in HBOT keloid tissue. But their regulatory relationship and mechanism in this process have not been investigated. Further work on this topic will be needed in the future.

In conclusion, HBOT can influence the expression of tumor immune gene and then induce immune cell infiltration variation in keloid tissue. CD80, ITGAM, IL-4, and PTPRC may be the key genes and activated memory $CD4^+$T lymphocyte cell may be the key regulatory cell in this process. Their relationship and regulatory mechanism need to be further investigated.

Funding

This study was supported by a grant from the National Natural Science Foundation of China (No. 81871538).

Conflicts of interest

None.

References

1. Marneros AG, Norris JE, Olsen BR, Reichenberger E. Clinical genetics of familial keloids. Arch Dermatol 2001;137:1429–1434. doi: 10.1001/archderm.137.11.1429.
2. Marneros AG, Norris JEC, Watanabe S, Reichenberger E, Olsen BR. Genome scans provide evidence for keloid susceptibility loci on chromosomes 2q23 and 7p11. J Investig Dermatol 2004;122:1126–1132. doi: 10.1111/j.0022-202X.2004.22327.x.
3. Ogawa R. Keloid and hypertrophic scars are the result of chronic inflammation in the reticular dermis. Int J Mol Sci 2017;18:606. doi: 10.3390/ijms18030606.
4. Shi CK, Zhao YP, Ge P, Huang GB. Therapeutic effect of interleukin-10 in keloid fibroblasts by suppression of TGF-(/Smad pathway. Eur Rev Med Pharmacol Sci 2019;23:9085–9092. doi: 10.26355/eurrev_201910_19311.
5. Diaz A, Tan K, He H, Xu H, Cueto I, Pavel AB, *et al*. Keloid lesions show increased IL-4/IL-13 signaling and respond to Th2-targeting-dupilumab therapy. J Eur Acad Dermatol Venereol 2020;34:e161–e164. doi: 10.1111/jdv.16097.
6. Bloch EF, Hall MG Jr, Denson MJ, Slay-Solomon V. General immune reactivity in keloid patients. Plast Reconstr Surg 1984;73:448–451. doi: 10.1097/00006534-198403000-00020.
7. Jin Q, Gui L, Niu F, Yu B, Lauda N, Liu J, *et al*. Macrophages in keloid are potent at promoting the differentiation and function of regulatory T cells. Exp Cell Res 2018;362:472–476. doi: 10.1016/j.yexcr.2017.12.011.
8. Lee YS, Liang YC, Wu P, Kulber DA, Tanabe K, Chuong CM, Widelitz R, Tuan TL. STAT3 signalling pathway is implicated in keloid pathogenesis by preliminary transcriptome and open chromatin analyses. Exp Dermatol 2019;28:480–484. doi: 10.1111/exd.13923.
9. Loh CY, Arya A, Naema AF, Wong WF, Sethi G, Looi CY. Signal Transducer and Activator of Transcription (STATs) proteins in cancer and inflammation: functions and therapeutic implication. Front Oncol 2019;9:48. doi: 10.3389/fonc.2019.00048.
10. Song KX, Liu S, Zhang MZ, Liang WZ, Liu H, Dong XH, *et al*. Hyperbaric oxygen therapy improves the effect of keloid surgery and radiotherapy by reducing the recurrence rate. J Zhejiang Univ Sci B 2018;19:853–862. doi: 10.1631/jzus.B1800132.
11. Zhang M, Liu S, Guan E, Liu H, Dong X, Hao Y, *et al*. Hyperbaric oxygen therapy can ameliorate the EMT phenomenon in keloid tissue. Medicine (Baltimore) 2018;97:e11529. doi: 10.1097/MD.0000000000011529.
12. Li WB, Liu S, Zhang MZ, Liu H, Dong XH, Hao Y, *et al*. Hyperbaric oxygen therapy relieved pruritus and pain of keloid patients. Am J Transl Res 2020;12:574–582.
13. Hao Y, Dong X, Zhang M, Liu H, Zhu L, Wang Y. Effects of hyperbaric oxygen therapy on the expression levels of the inflammatory factors interleukin-12p40, macrophage inflammatory protein-1β, platelet-derived growth factor-BB, and interleukin-1 receptor antagonist in keloids. Medicine (Baltimore) 2020;8:360. doi: 10.1097/MD.0000000000019857.
14. Wolfram D, Tzankov A, Pülzl P, Piza-Katzer H. Hypertrophic scars and keloids - a review of their pathophysiology, risk factors, and therapeutic management. Dermatol Surg 2009;35:171–181. doi: 10.1111/j.1524-4725.2008.34406.x.
15. Limandjaja GC, Niessen FB, Scheper RJ, Gibbs S. The keloid disorder: heterogeneity, histopathology, mechanisms and models. Front Cell Dev Biol 2020;99:e19857. doi: 10.3389/fcell.2020.00360.
16. Ladin DA, Hou Z, Patel D, McPhail M, Olson JC, Saed GM, *et al*. P53 and apoptosis alterations in keloids and keloid fibroblasts. Wound Repair Regen 1998;6:28–37. doi: 10.1046/j.1524-475x.1998.60106.x.
17. Suzuki M, Yokota M, Matsumoto T, Ozaki S. Synergic effects of CD40 and CD86 silencing in dendritic cells on the control of allergic diseases. Int Arch Allergy Immunol 2018;177:87–96. doi: 10.1159/000489862.
18. Fagerholm SC, Varis M, Stefanidakis M, Hilden TJ, Gahmberg CG. alpha-Chain phosphorylation of the human leukocyte CD11b/CD18 (Mac-1) integrin is pivotal for integrin activation to bind ICAMs and leukocyte extravasation. Blood 2006;108:3379–3386. doi: 10.1182/blood-2006-03-013557.
19. Nguyen JK, Austin E, Huang A, Mamalis A, Jagdeo J. The IL-4/IL-13 axis in skin fibrosis and scarring: mechanistic concepts and therapeutic targets. Arch Dermatol Res 2020;312:81–92. doi: 10.1007/s00403-019-01972-3.
20. Hermiston ML, Xu Z, Weiss A. CD45: a critical regulator of signaling thresholds in immune cells. Annu Rev Immunol 2003;21:107–137. doi: 10.1146/annurev.immunol.21.120601.140946.
21. Murao N, Seino KI, Hayashi T, Ikeda M, Funayama E, Furukawa H, *et al*. Treg-enriched CD4+ T cells attenuate collagen synthesis in keloid fibroblasts. Exp Dermatol 2014;23:266–271. doi: 10.1111/exd.12368.
22. Faleo G, Fotino C, Bocca N, Molano RD, Zahr-Akrawi E, Molina J, *et al*. Prevention of autoimmune diabetes and induction of (-cell proliferation in NOD mice by hyperbaric oxygen therapy. Diabetes 2012;61:1769–1778. doi: 10.2337/db11-0516. Epub 2012 May 7.
23. Buras JA, Holt D, Orlow D, Belikoff B, Pavlides S, Reenstra WR. Hyperbaric oxygen protects from sepsis mortality via an interleukin-

10-dependent mechanism. Crit Care Med 2006;34:2624–2629. doi: 10.1097/01.CCM.0000239438.22758.E0.
24. Shapira R, Solomon B, Efrati S, Frenkel D, Ashery U. Hyperbaric oxygen therapy ameliorates pathophysiology of 3xTg-AD mouse model by attenuating neuroinflammation. Neurobiol Aging 2018;62:105–119. doi: 10.1016/j.neurobiolaging.2017.10.007.
25. Wang ZC, Zhao WY, Cao Y, Liu YQ, Sun Q, Shi P, *et al*. The roles of inflammation in keloid and hypertrophic scars. Front Immunol 2020;11:603187. doi: 10.3389/fimmu.2020.603187.
26. Wilgus TA, Ud-Din S, Bayat A. A review of the evidence for and against a role for mast cells in cutaneous scarring and fibrosis. Int J Mol Sci 2020;21:9673. doi: 10.3390/ijms21249673.
27. Betarbet U, Blalock TW. Keloids: a review of etiology, prevention, and treatment. J Clin Aesthet Dermatol 2020;13:33–43.
28. Zhang Q, Yamaza T, Kelly AP, Shi S, Wang S, Brown J, *et al*. Tumor-like stem cells derived from human keloid are governed by the inflammatory niche driven by IL-17/IL-6 axis. PLoS One 2009;4:e7798. doi: 10.1371/journal.pone.0007798.

How to cite this article: Wang CH, Shan MJ, Liu H, Hao Y, Song KX, Wu HW, Meng T, Feng C, Qi Z, Wang Z, Wang YB. Hyperbaric oxygen treatment on keloid tumor immune gene expression. Chin Med J 2021;134:2205–2213. doi: 10.1097/CM9.0000000000001780